Available online at www.sciencedirect.com
SCIENCE DIRECT®
Biosensors and Bioelectronics 19 (2004) 1765–1774
BIOSENSORS & BIOELECTRONICS
www.elsevier.com/locate/bios

Erratum

Dielectrophoretic registration of living cells to a microelectrode array☆

Darren S. Gray[a], John L. Tan[a], Joel Voldman[b], Christopher S. Chen[a,*]

[a] *Department of Biomedical Engineering, Johns Hopkins University School of Medicine, 720 Rutland Avenue, Baltimore, MD 21205, USA*
[b] *Department of Electrical Engineering and Computer Science, Massachusetts Institute of Technology, Cambridge, MA 02139, USA*

Abstract

We present a novel microfabricated device to simultaneously and actively trap thousands of single mammalian cells in alignment with a planar microelectrode array. Thousands of 3 μm diameter trapping electrodes were fabricated within the bottom of a parallel-plate flow chamber. Cells were trapped on the electrodes and held against destabilizing fluid flows by dielectrophoretic forces generated in the device. In general, each electrode trapped only one cell. Adhesive regions were patterned onto the surface in alignment with the traps such that cells adhered to the array surface and remained in alignment with the electrodes. By driving the device with different voltages, we showed that trapped cells could be killed by stronger electric fields. However, with weaker fields, cells were not damaged during trapping, as indicated by the similar morphologies and proliferation rates of trapped cells versus controls. As a test of the device, we patterned ~20,000 cells onto a 1 cm^2 grid of rectangular adhesive regions, with two electrodes and thus two cells per rectangle. Our method obtained 70 ± 1% fidelity versus 17 ± 1% when using an existing cell-registration technique. By allowing the placement of desired numbers of cells at specified locations, this approach addresses many needs to manipulate and register cells to the surfaces of biosensors and other devices with high precision and fidelity.

Keywords: Dielectrophoresis; Endothelial cells; Microfabrication; Array; Biosensor; Patterning

1. Introduction

Cell-based biosensors, where living cells comprise the primary sensing elements, are well suited for detection of chemical- and biological-warfare agents and for rapid drug screening (Pancrazio et al., 1999; Stenger et al., 2001). The natural ability of cells to respond to biological inputs in a physiological manner allows for detection of relevant compounds in complex environments, with or without determining the identities or mechanisms of action of the active agents (Pancrazio et al., 1999; Stenger et al., 2001). For the efficient, parallel analysis of drug candidates, cell-based systems offer reduced cost and complexity compared with animal models (Bhadriraju and Chen, 2002).

A primary challenge involved in constructing cell-based devices is achieving and maintaining precise positioning of a controlled number of cells in registration with analytic components on a microchip (Pancrazio et al., 1999). Several groups have successfully interfaced various types of cells with sensing and detecting elements to form cell-based biosensors (Pancrazio et al., 1999, Stenger et al., 2001). However, currently methods do not exist to safely and efficiently align single cells with detection elements in large arrays in order to facilitate signal transmission and prevent misplaced cells from interfering with other components. For sensors with outputs proportional to cell number, the ability to predetermine this quantity greatly simplifies data analysis. Ideally, cells would be seamlessly integrated into devices with a method to prescribe their numbers and locations, much as the layout of other components is specified.

Two recently developed techniques that can organize large numbers of cells on surfaces are based on patterned adhesiveness and microfluidic patterning (Kane et al., 1999). In the first case, cells are randomly distributed onto a surface containing adhesive and nonadhesive regions. Cells that happen to settle on the adhesive regions attach to the surface, while cells on nonadhesive regions are rinsed away. With microfluidics, cells are confined to certain streams of laminar flow and, therefore, a subset of the sensor surface. Both methods can be used as registration tools, but neither can control the placement of individual cells. To achieve single-cell resolution, cells can be placed one at a time using a variety of physical or optical manipulation tools (Skerman,

☆ doi of original article 10.1016/j.bios.2003.08.013.
* Corresponding author. Tel.: +1-410-614-8624; fax: +1-410-955-0549.
E-mail address: cchen@bme.jhu.edu (C.S. Chen).

0956-5663/$ – see front matter © 2004 Elsevier B.V. All rights reserved.
doi:10.1016/j.bios.2004.03.016

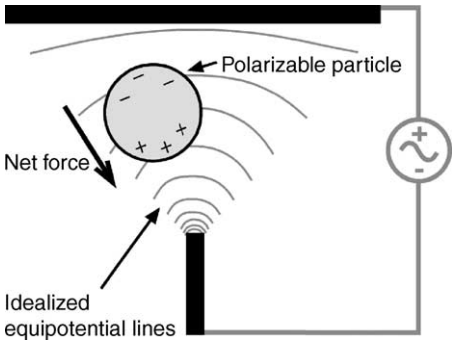

Fig. 1. Theory of DEP. A particle that is more polarizable than the surrounding media is pushed toward a field maximum, where the electrical equipotential lines are closest together. A net dielectrophoretic force upon the particle (F_{DEP}) occurs because of an inequality between the coulombic forces acting upon the two halves of the particle. Note that when the signs of the voltages are reversed under AC conditions, the induced dipole reverses, but the particle feels the same net force.

1968; Ashkin et al., 1987; Jager et al., 2000), but the sacrifice in throughput limits these approaches to specialized applications.

A preferred cell-registration technique would safely and rapidly place many cells at arbitrary locations with single-cell resolution. Cells would then maintain their positions after they adhered and spread on the surface. We have developed an active positioning system that meets these requirements. Cells are trapped using dielectrophoresis (DEP), the force on polarizable bodies in a nonuniform electric field (Pohl, 1978; Jones, 1995) (Fig. 1). Previous studies have used DEP to sort groups of cells based on their electrical characteristics (Pethig, 1996) or to temporarily trap and examine single cells (Voldman et al., 2002), but not to generate 2D arrays of individual cells. In our system, the cells are more polarizable than the surrounding media, so dipoles induced in the cells align parallel to the applied electric field (Pohl, 1978; Jones, 1995). Because the field is spatially nonuniform, a resultant force due to DEP pulls the cells towards field maxima (Pohl, 1978; Jones, 1995). These maxima occur at electrodes embedded within a flat substrate (microchip) surface. When the polarity of the applied field is reversed, DEP continues to pull the cell towards the field maximum, allowing AC operation at high frequencies to reduce electrical loading of the cell membrane (Glasser and Fuhr, 1998). After a cell has been trapped at a field maximum, other cells can also be pulled towards that maximum, albeit more weakly. Fluid flow across the surface is used as a destabilizing force to remove these additional cells. Single-cell positioning is implemented by using flows that are powerful enough to remove the additional cells but too weak to remove the strongly trapped cell directly above each electrode. Using standard microfabrication techniques, thousands of trapping electrodes can be embedded over a single square centimeter portion. The entire array of single cells is formed within several minutes.

Once cells adhere to a microchip, they can migrate away from their original positions by exerting forces (Galbraith and Sheetz, 1999; Balaban et al., 2001; Tan et al., 2003) much greater than those applied by DEP (Hughes and Morgan, 1999; Voldman et al., 2001). To address this issue, we used an additional technique to maintain the positions of motile cells after they adhered. This confinement was accomplished by aligning a pattern of cell-adhesive regions with the electrode array, surrounded by a nonadhesive coating. Thus, after trapping with DEP, cells attached to the adhesive pattern and remained aligned to the electrodes. The combination of DEP and adhesive regions allowed us to produce and maintain large arrays of individual, aligned cells, which could be used in many biosensor applications.

2. Materials and methods

2.1. Modeling and calculations

Electric fields were modeled using FlexPDE version 3 (PDE Solutions Inc, USA), a finite element package, to solve the Laplace equation. We assumed permittivity-dominated operation, as justified by both analytical calculations and the existence of the DC-blocking silicon dioxide layer. The boundary conditions imposed were continuity between different materials and the presence of the applied voltage throughout the metal regions. A two-dimensional model was sufficient to describe the system, based on the rotational symmetry of the round traps, which we would expect to yield similar electric fields in any plane perpendicular to the plane of the array of traps. Approximate dielectric constants (relative permittivities) used for modeling the media, photoresist, and silicon dioxide were 80, 4, and 4, respectively (Sears et al., 1980; Sison et al., 1995; Murray, 1997), assuming that the media and the photoresist had dielectric constants similar to that of water and other novolac-based positive photoresists, respectively. Media conductivity was measured with a conductivity meter (116, Thermo Electron, USA), and cell radius was measured using a sizing counter (Z2, Beckman Coulter, USA).

2.2. Fabrication of substrates

To construct DEP substrates, 22 mm × 60 mm #1.5 coverslips were rinsed with ethanol, and then coated with a 50 Å layer of titanium followed by a 150 Å one of gold, using an electron beam evaporator (Sharon Vacuum, USA). The gold layer was spin-coated with a ∼1.5 μm thick layer of S1813 positive photoresist (Shipley, USA) and patterned photolithographically as previously described (Kane et al., 1999), leaving 3 μm diameter holes in the photoresist layer. To form trapping electrodes, additional gold was electroplated with a current density of 1 mA/cm^2 using a non-cyanide plating solution (Techni Gold 25E, Technics, Inc., USA) onto gold regions not covered by photoresist. This process was continued until the electroplated gold electrodes reached the height of the photoresist, as determined by

periodic inspection under a metallurgy microscope (Eclipse ME600, Nikon, Japan) with a 50× objective. Substrates were baked at 160 °C and simultaneously illuminated with 1.5 mW/cm^2 of broadband UV light for 6 min to achieve non-toxicity by removing residual solvent from the photoresist and improve its mechanical robustness through further cross-linking. Next, a 200 Å thick layer of silicon dioxide was deposited onto the substrates by electron beam evaporation. Substrates were then plasma-oxidized for l min (Plasma Prep II, Structure Probe, Inc., USA) and treated with a vapor of tri-decafluoro-1,1,2,2-tetrahydrooctyl-1-trichlorosilane (United Chemical Technologies, USA) to enhance protein adsorption by increasing surface hydrophobicity.

2.3. Patterning adhesiveness of substrates

To register cell adhesiveness onto the DEP electrode surface, fibronectin location on substrates was patterned using membranes constructed as described elsewhere (Jackman et al., 1999). Membranes, consisting of a layer of epoxy which minimized distortion and a layer of silicone elastomer which sealed hydrophobically against substrate surfaces, were aligned to substrates using a mask aligner (MJB-3, Karl Suss, Germany). Fibronectin was adsorbed at 100 μg/ml in PBS onto substrates through holes in the membranes for 1 h, and then rinsed three times with ddH_2O. After membranes were removed, 2 mg/ml Pluronics F127 (BASF, Germany) was adsorbed for 1 h to coat the regions previously masked by membranes, rinsed three times with ddFkO, and dried. To make substrates uniformly coated with adhesive, 100 μg/ml fibronectin was adsorbed onto the entire surfaces of substrates for 1 h, rinsed three times with ddH_2O, and dried.

Non-electrode substrates were patterned with fibronectin as follows. Fibronectin at 100 μg/ml in PBS was adsorbed onto PDMS (Sylgard 184, Dow Corning, USA) stamps made as previously described (Kane et al., 1999). The fibronectin was rinsed three times with deionized water and dried with nitrogen before being stamped onto flat PDMS substrates, which were previously oxidized for 7 min in a UV-ozone cleaner (342, Jelight, USA). Substrate regions not stamped with fibronectin were rendered nonadhesive by the adsorption of 2 mg/ml Pluronics F127 (BASF, Germany) for 1 h. Substrates were rinsed three times with deionized water before use.

2.4. Flow chamber and electronics

A custom-built parallel-plate flow chamber similar to that previously described (Voldman et al., 2001) was used to introduce cells to substrates and provide the destabilizing flow to remove extra cells. Our chamber includes a 150 Å thick, transparent gold counterelectrode deposited onto the Plexiglas chamber lid by electron beam evaporation. The floor of the chamber consists of the substrate itself, and a silicone gasket forms the walls of the chamber. The chamber height, width, and length are 160 μm, 1.5 cm, and 4 cm, respectively. Fluids were introduced into the system from 3 ml syringes via 1/16 in. i.d. tubing. A four-way valve (V-101D, Upchurch, USA) was used to switch between fluids without introducing bubbles into the system. The chamber was sterilized with ethanol and dried before each use.

To substrates and the counterelectrode were applied AC voltages used to produce nonuniform electric fields, using circuitry similar to that previously described (Voldman et al., 2001). In our circuit, output amplifiers (LM6321, National Semiconductor, USA) were added as a last circuit stage to provide increased output current and waveform stability. Substrates were energized with a sinusoidal waveform at 0, 5, or 10 Vpp and 2 MHz, while the counterelectrode was energized with a similar waveform shifted in phase by 180°.

2.5. Cell culture and reagents

Bovine pulmonary arterial endothelial cells (BPAECs, VEC Technologies, USA) and NIH/3T3 fibroblasts (3T3s, ATCC, USA) were cultured at 37 °C under humidified 10 and 5% Co_2/air atmospheres, respectively. Cells were cultured in Dulbecco's Modified Eagle Medium (Invitrogen, USA) supplemented with 10% calf serum, 100 U/ml penicillin, and 100 μg/ml streptomycin (DMEM/CS). Prior to plating on DEP substrates, cells were detached using 0.25% trypsin and 1 mM ethylenediaminetetraacetic acid in PBS (300 mOsm, Invitrogen, USA), rinsed with 22 μg/ml Soybean trypsin inhibitor (Invitrogen, USA) in DMEM/CS, pelleted by centrifugation at 240 × g for 4 min, resuspended in 3 ml of 300 mOsm sucrose with 1% calf serum (sucrose media), vacuum degassed for 3 min, and pulled into syringes already containing 1 ml of 10% CO_2/air. Cells plated on non-electrode substrates were resuspended in DMEM/CS immediately after trypsinization.

2.6. Dielectrophoresis operation

Before cells were introduced to the flow chamber containing an electrode substrate, the system was flushed with 2–4 volumes of vacuum-degassed sucrose media. Flow from syringes into the flow chamber was produced either by hand or by a syringe pump (KDS-210, KD Scientific, USA). After cells began to flow over the substrate, as monitored with a microscope, the system was energized with 5 V at 2 MHz. Flow continued at approximately 50 μl/min for 5 min, as single and multiple cells were trapped on electrodes. The incoming fluid was then switched to sucrose media without cells, and flow was increased to approximately 150 μl/min for 5 min, in order to remove extra cells from electrodes. The flow chamber was then placed at 37 °C, and cells were allowed to adhere to the substrate for 20 min with a flow rate of 20 μl/min. After the flow chamber was opened by gently lifting the lid upwards, substrates and adhered cells were aseptically removed and placed in standard culture media.

2.7. Microscopy

Phase-contrast and fluorescence images of cells were taken using a cooled CCD camera (Orca 100, Hamamatsu, Japan) attached to an inverted microscope (Eclipse TE200, Nikon, Japan) with a 10× objective. Images represented regions of approximately 900 μm × 700 μm.

2.8. Cellular assays

To measure acute cell damage, 2 μg/ml propidium iodide (Molecular Probes, USA) was added to the media. Bright fluorescence of cells due to propidium iodide uptake indicated a loss of cell membrane integrity. Three sets of fluorescence and phase-contrast images were taken per timepoint at each voltage during three separate trials with three different substrates. Percent cell viability was calculated as $100 \times (T - D)/T$, where T represents the total number of cells counted in the phase-contrast image and D represents the number of damaged cells.

To assess proliferation, cells were counted from four phase-contrast images of each substrate 1.5, 24, and 48 h after DEP or random seeding during each of three separate trials, using a new DEP substrate and a new randomly seeded substrate for each trial. These images, as well as live viewing, were also used to qualitatively assess cell morphology, including size, shape, vesicles, and potential blebbing.

To measure the degree of registration between cells and substrates, four sets of phase-contrast and immunofluorescence images were taken 1–2 h after DEP or random seeding during each of four separate trials of DEP and three separate trials of random seeding, all with different substrates. Cells were counted manually from these images, and correct alignment of cells was scored as the percentage of adhesive regions containing two cells.

To visualize fibronectin and nuclei, samples were fixed for 20 min in PBS containing 4% formaldehyde, washed three times in IF buffer (PBS containing 0.1% BSA and 0.1% Triton X-100), and blocked overnight in IF buffer. Substrates were then incubated for 60 min in IF buffer containing 130 μg/ml fluorescein-conjugated goat anti-human fibronectin antibody (#55193, ICN Biomedicals, Inc., USA) and 4 μg/ml Hoechst 33258 (Molecular Probes, USA) to stain for fibronectin and nuclei, respectively, and then rinsed three times in IF buffer.

3. Results

3.1. Finite element modeling and determination of system parameters

Finite element modeling (FEM) was used to evaluate the theoretical dependence of electric field on substrate geometry (Fig. 2A and B). To arrive at a substrate geometry capable of producing the nonuniform electric fields suitable for trapping cells, several parameters of the design (Fig. 2A) were

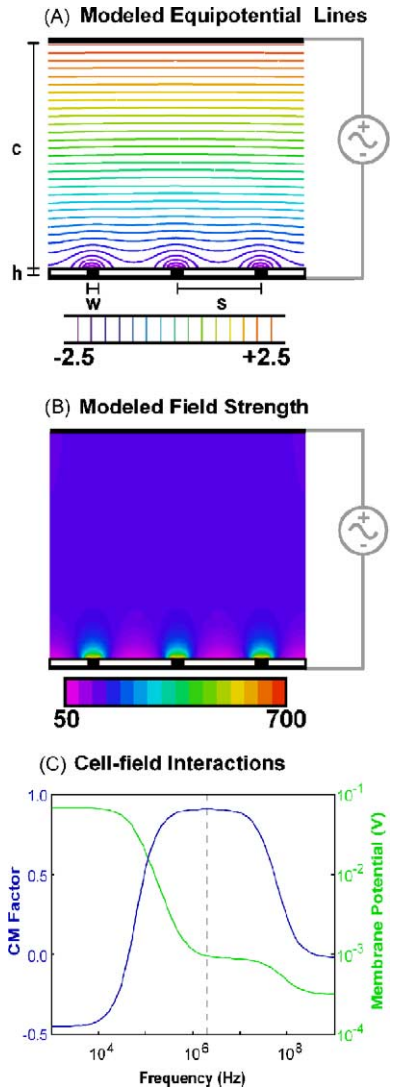

Fig. 2. Modeling of DEP in "points-and-lid" geometry. (A) Calculated equipotential lines, based on an applied potential of 5 Vpp at 2 MHz, are shown for a group of three traps. Electric potential is illustrated by a linear color scale from −2.5 to +2.5 V. Trap height, trap width, trap spacing, and chamber height are indicated by h, w, s, and c, respectively. The parameters used for the final design were $h = 1.5$, $w = 3$, $s = 30$, and $c = 160$ μm. (B) Calculated electric field strength is illustrated with a linear color scale from 50 to 700 kV/m. Force due to DEP is proportional to the gradient of the square of the field strength. (A, B) Electric field was modeled using a finite element package (FlexPDE 3, PDE Solutions, Inc., USA). The illustrations represent traps with height h of 1.5 μm, width w of 3 μm and spacing s of 20 μm, the minimum spacing able to trap single cells. For convenient presentation, the chamber height c represents only 55 μm. Simulations using the actual height of 160 μm yielded similar results (data not shown). Drawings are to scale, except for the uniform "lid" counterelectrode and the gold layer connecting the traps; both are shown with increased thickness. The silicon dioxide passivation layer was included in the simulation, but its thickness to scale is less than the linewidth used in this figure. (C) Plot of the real part of the Clausius–Mossotti Factor (CM Factor) and maximum transmembrane voltage (membrane potential) with an applied potential of 5 V and the geometric parameters used in experiments. An operating frequency of 2 MHz was chosen to maximize CM, and thus dielectrophoretic force, in a region of acceptably low transmembrane potential. Dotted line indicates 2 MHz.

varied. In FEM, the gradient of the square of the electric field intensity adjacent to the trapping electrode was used as a measure of trap strength. In experiments, trap strength was assumed to be proportional to the flow rate required to remove a single cell from a trap. The strength of modeled traps varied directly with trap height h when this parameter was much less than trap width w but was unaffected by h at larger values of h. One would expect this result, since at large h values the contribution of the metal layer underlying the electrodes becomes negligible, and thus the distance of this layer from the inside of the flow chamber becomes unimportant. Inversely, as $h \rightarrow 0$, the model approaches the case in which the electric field is uniform, and thus no DEP occurs. Using h values on the order of w or greater, experiments showed no significant changes in trap strength with changes in h (data not shown). A trap height of 1.5 μm was chosen for ease of manufacture. FEM also showed that trap strength increased in proportion to trap width w. This trend was confirmed experimentally (data not shown). However, smaller traps were more effective at trapping single cells due to stoichiometric exclusion of additional cells. A trap width of 3 μm provided an acceptable compromise and was used for this study. In FEM, trap spacing s had little effect on trap strength. In practice, the minimum useful trap spacing was approximately 20 μm, center to center. At a lower spacing, unwanted cells occasionally got lodged between trapped cells. A spacing of 30 μm was therefore used in this study. In FEM, trap strength decreased with increasing chamber height c, although using higher potentials could counterbalance this effect. Experimental trials verified this trend (data not shown). A chamber height of 160 μm was chosen for optimal flow and electrical characteristics.

After geometrical parameters were chosen based on FEM and experimentation, calculated interactions between cells and the electric field (Fig. 2C) were used to select the field frequency. The force on a round cell due to dielectrophoresis can be approximated as

$$F_{\mathrm{DEP}} = 2\pi\varepsilon R^3 \mathrm{Re}[\underline{\mathrm{CM}}(\omega) \times \nabla \underline{E}^2(R)], \quad (1)$$

where F_{DEP} refers to the force on the cell due to dielectrophoresis, ε is the permittivity of the surrounding media, R is the radius of the cell, CM is the Clausius–Mossotti factor, ω is the frequency of the applied electric field in radians, E is the applied electric field, and r denotes the spatial coordinates of the cell. We measured e and R as 20 mS/m and 6.25 μm, respectively. CM as a function of ω was calculated to the first order (Fig. 2C) using values from the literature (Huang et al., 1997) by modeling the cell as a sphere (cytoplasm) covered by a dielectric shell (cell membrane) (Jones, 1995).

On the basis of this calculation, we selected a frequency of 2 MHz to maximize the Clausius–Mossotti Factor, and thus the force of dielectrophoretic trapping. This frequency also exceeds the ∼400 kHz cutoff of the high-pass filter formed by the resistive media and the capacitative SiO_2, ensuring that a large percentage of the applied potential is actually available to produce DEP. Transmembrane voltage was calculated (Fig. 2C) using the above values and approximations along with the FEM-derived field strength at the center of the cell. Predicted loading of the cell membrane at 2 MHz is minimal and less than that tolerated in a previous work (Fuhr et al., 1994). With an applied potential of 5 V and the chosen frequency of 2 MHz, our calculations indicate that only 1 mV would be applied across the cell membrane.

3.2. Registration using dielectrophoresis

Substrates used to register cells via DEP were embedded with arrays of 3 μm electrodes, constructed using standard microfabrication techniques (Fig. 3). After substrates were placed in a parallel-plate flow chamber, cells in degassed sucrose media were introduced to the electrode surface (Fig. 4A) and visualized inside the transparent setup using an inverted microscope. Cells were not adversely affected by degassing for up to 15 min. A sinusoidal waveform with an amplitude of 5 V and a frequency of 2 MHz was applied to the electrodes, energized via a conductive layer below the substrate surface. A similar waveform, shifted in phase by 180°, was applied to a uniform counterelectrode forming the lid of the chamber. Cells were trapped on the substrate surface at potential energy wells created by the nonuniform electric field (Fig. 4B). When a cell was <15 μm from an unfilled trap, it would typically move to the trap in less than 1 s. Cells further from electrodes were usually not trapped unless flow was halted. The entire 1 cm × 1 cm array was filled with cells within 5 min.

Fluid flow was then increased, providing a destabilizing force to reduce the potential energy wells to the size of single cells, preventing multiple cells from remaining at a given trap (Fig. 4C). Flows of 100–500 μm/min left single cells in traps, while flows below this range left multiple cells, and greater flows removed single cells from traps. Destabilization with suitable fluid flow was highly effective at removing multiple cells from traps except when groups of two or more cells entered the flow chamber already attached to each other. These clumps of cells, especially those containing two cells, could not usually be separated by flow.

Within 10–15 min, cells adhered to the surface. Most cells remained round and did not spread on the surface in the presence of the sucrose media used to perform DEP. While cells seemed to tolerate exposure to sucrose media for at least 1 h, those left in sucrose overnight detached more frequently and proliferated more slowly than controls (data not shown). In the registration experiments, cells resumed normal spreading when substrates were removed from the flow chamber and placed in standard culture media. After cells spread on the substrate surface, aligned adhesive regions surrounding the traps restricted cell migration (Fig. 4D).

3.3. Assessment of cell health

Mammalian cells are fragile and easily damaged by a variety of physical forces. Although previous work has shown

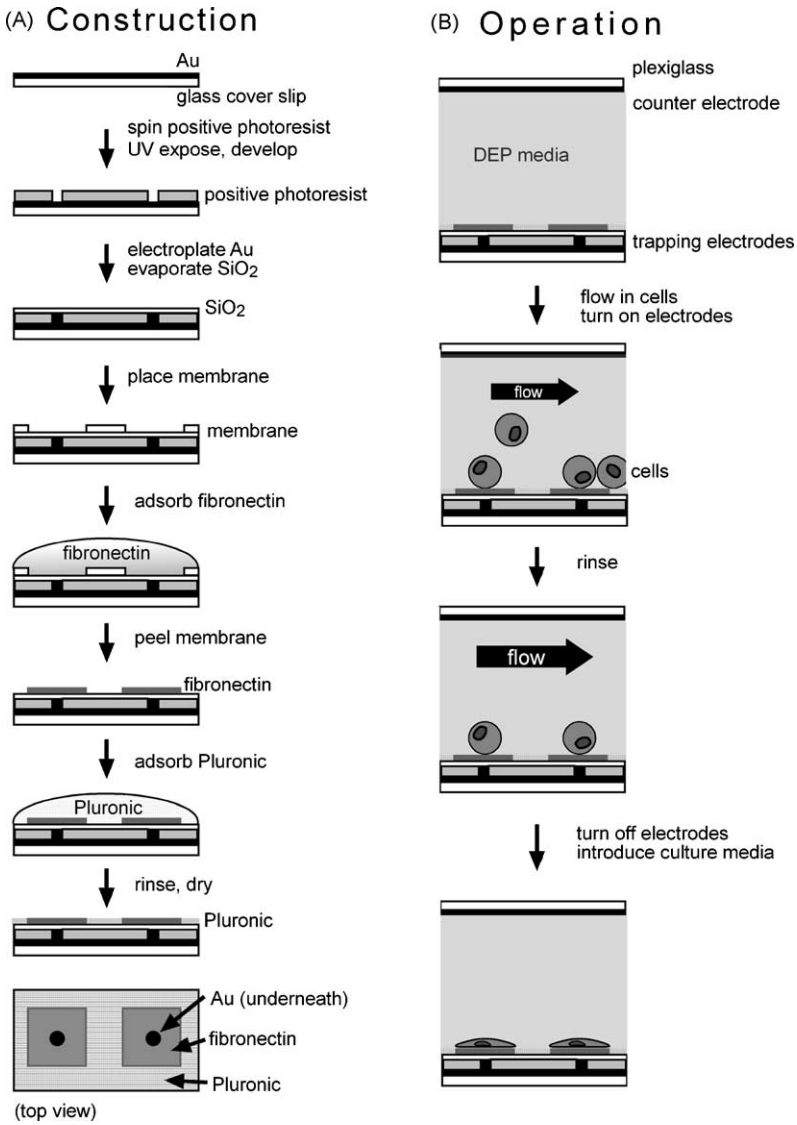

Fig. 3. (A) Construction of the DEP substrates. All views are depicted as side views; the final construction is depicted also as a top view, (B) Operation of the DEP patterning system, with substrates placed in a parallel-plate flow chamber. Construction and operation are described further in Section 2. Drawings are not to scale.

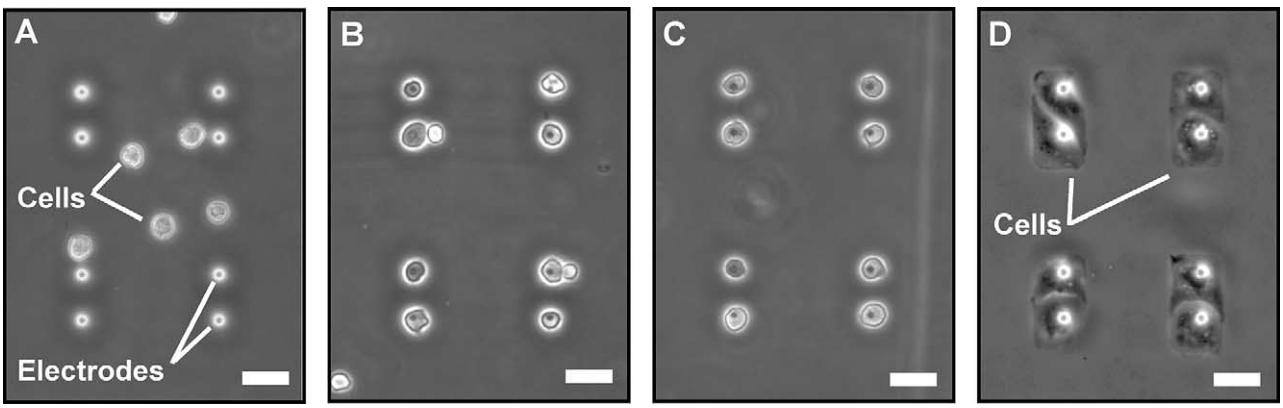

Fig. 4. Photographs of various stages of the dielectrophoretic patterning of cells. (A) Randomly distributed cells with electrodes turned off. (B) With a fluid flow rate of ~50 μl/min, energized traps attract single and multiple cells. (C) With fluid flow at the rate of ~150 μl/min, single cells remain trapped while additional cells are removed. (D) Cells spread on the adhesive regions 1 h after DEP. In (B) and (C), flow is from left to right. Scale bars are 30 μm.

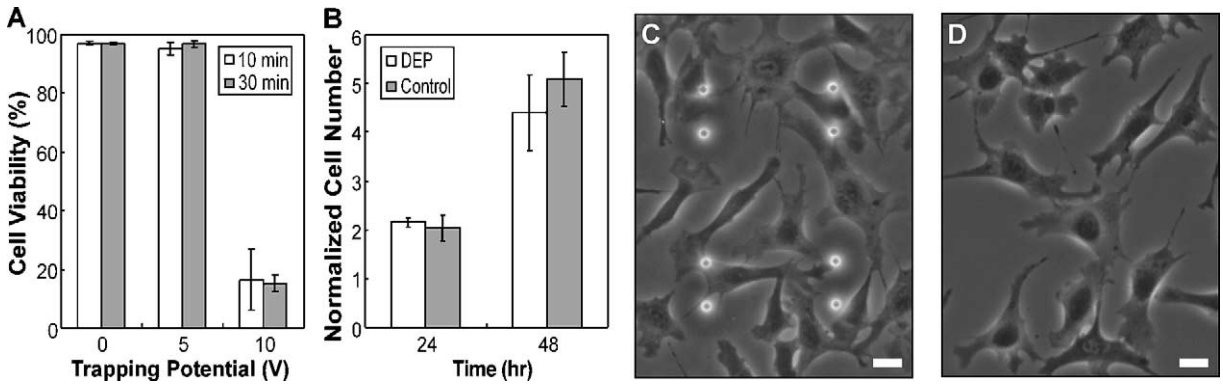

Fig. 5. Analysis of the effects of DEP on cell health. (A) The acute effect of the electric field on cell viability. Cells were considered viable if they did not fluoresce due to propidium iodide uptake. (B) Proliferation rates of cells exposed to DEP vs. tissue culture controls. (C, D) Photographs illustrating the morphology of representative cells 24 h after seeding with (C) or without (D) DEP. Trapping electrodes can be seen in (C) but were not present in (D). In (C), the cells outnumber the electrodes due to cell proliferation, and are not localized to the electrodes because these substrates are uniformly adhesive. Normalized cell number is calculated as cells per unit area at a given time divided by cells per unit area 90 min after cell seeding. Error bars are standard error. Scale bars are 30 μm.

DEP to be a safe method for manipulation of cells (Glasser and Fuhr, 1998; Archer et al., 1999; Docoslis et al., 1999; Heida et al., 2001), and our calculations suggest acceptable transmembrane potentials (Fig. 2C), these results do not rule out the possibility that our setup could have caused cellular injury. To assay for immediate damage to cells undergoing DEP, BPAECs were incubated with propidium iodide, a common viability indicator previously used to detect electrical damage to cells (Djuzenova et al., 1996). While intact cells are impermeable to this fluorescent dye, it enters and binds the nucleic acids of cells having compromised cell membranes. Thus, damaged cells fluoresce brightly and can be easily distinguished from unstained, healthy cells. To determine the voltage level that cells could withstand over a duration sufficient for trapping, we subjected cells in the DEP apparatus to 0, 5, or 10 V at 2 MHz over 30 min. Cells could be subjected to at least 5 V for the entire 30 min without a significant increase in damage relative to controls at 0 V (Fig. 5A). Most cells subject to 10 V or more were damaged within 10 min. To maintain cell viability and surpass the minimum 3 V needed to trap cells, we used 5 V trapping potentials for further experiments.

To assay for more subtle and less acute changes in the health of cells subject to DEP, we analyzed proliferation (growth) rate and morphology, both of which are broadly indicative of cell health (Freshney, 2000). BPAECs were trapped on uniformly adhesive electrode arrays by exposure to DEP at 5 V and 2 MHz for 30 min, and then monitored for 2 days in culture. Our results indicate that the proliferation rate of cells undergoing DEP was not significantly different from control cells grown under standard tissue culture conditions (Fig. 5B). The morphologies of DEP cells were also similar to controls over this time period (Fig. 5C and D). We noted no differences in size, shape, vesicles, or blebbing.

3.4. Evaluation of cell registration

In order to compare DEP trapping with registration via patterned adhesiveness alone, we simulated a biosensor in which two cells per sensor were desired on thousands of 30 μm × 60 μm sensors, spaced 60 μm apart in a 1 cm × 1 cm array. For DEP trials, substrates consisted of 30 μm × 60 μm adhesive regions, each containing two electrical traps. For patterned adhesiveness alone, substrates consisted of adhesive regions without electrical traps. In a preliminary trial of adhesiveness alone, a cell density of approximately 10^4 cells/cm^2 was found to produce the most adhesive regions with two adherent cells. This seeding density was used for quantified trials of adhesiveness alone. To quantitate the two registration methods, BPAECs were either seeded randomly onto adhesive regions or trapped using DEP. For trials with and without DEP, adhesive regions were scored as “correct” if they contained two cells 1–2 h after patterning. With DEP, 70 ± 1% of regions were correct over four trials (Fig. 6A and C), while three trials with adhesiveness alone yielded only 17 ± 1% correct regions (Fig. 6B and D). Similar trapping was achieved with NIH/3T3 fibroblasts.

4. Discussion

We have demonstrated a method to control the placement of individual cells in order to reliably integrate cells into various sensors and other devices. The ability to register cells with detection elements could facilitate increased integration of cells with various devices by allowing the number and location of cells to be specified much like other components. Tight control over the placement of cells is expected to improve the sensitivity and signal-to-noise ratio in many cell-based sensors. Because DEP is electrically driven, it is inherently well suited for interfacing with electronics and

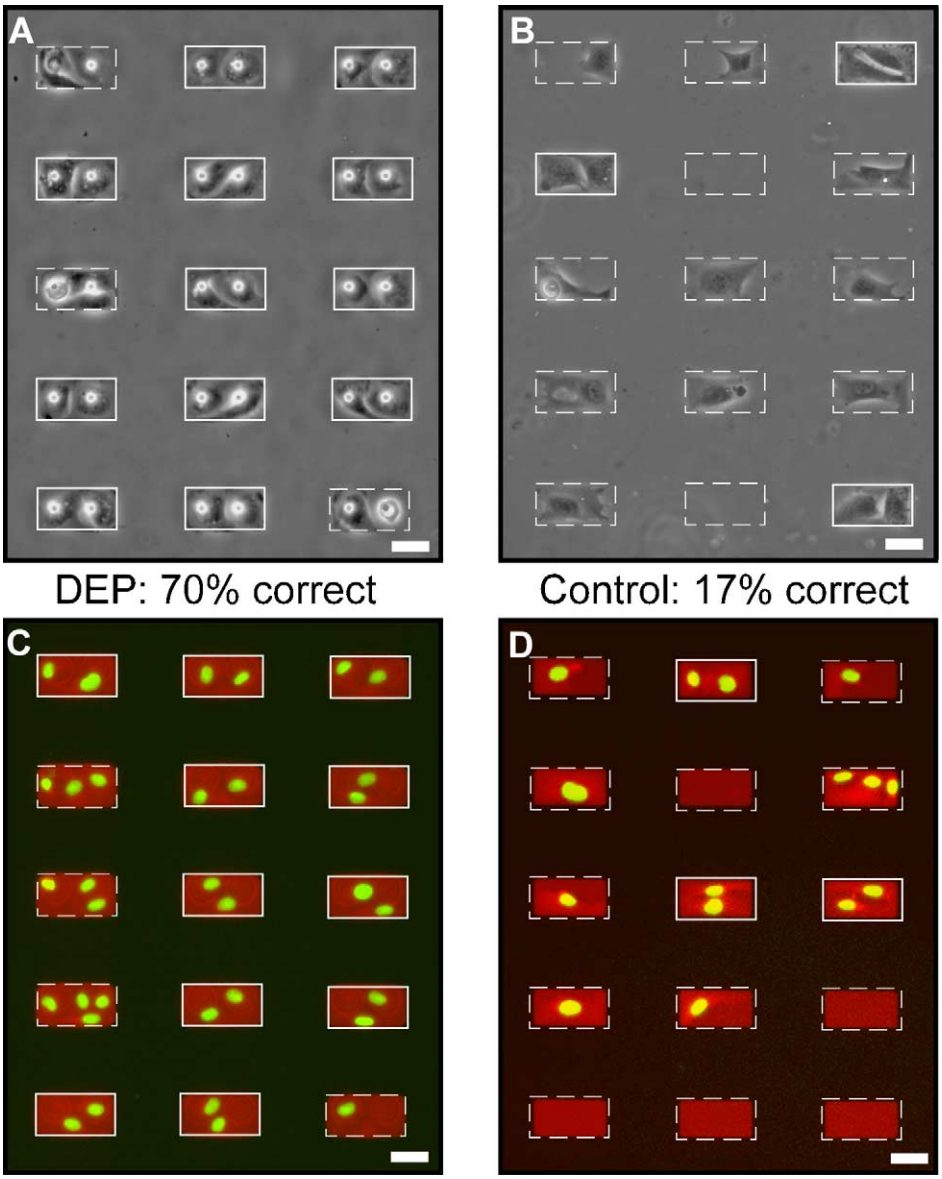

Fig. 6. Fidelity of cell patterning on ECM islands with (A, C) and without (B, D) DEP. "Correct" islands are defined as islands containing two cells 1–2 h after patterning. Correct islands are outlined with solid lines, while incorrect islands are outlined with dotted lines. In (B) and (D), fluorescence micrographs show nuclei in green and adhesive fibronectin in red. Nuclei and fibronectin were stained with Hoechst dye and a fluorescein-conjugated anti-fibronectin antibody, respectively. All photos represent different regions. Islands on substrates patterned with DEP were $70 \pm 1\%$ correct ($n = 4$), while $17 \pm 1\%$ of islands were patterned correctly at optimal seeding density without DEP ($n = 3$). Scale bars are 30 μm.

computer control, and the trapping electrodes could even be used to receive cellular signals during biosensor operation. The "points-and-lid" geometry used in this paper allows the creation of nearly arbitrary geometric patterns. Because the electrodes in our novel geometry can be connected to a single bus layer within the substrate, they do not require individual wiring. Scale-up of the array beyond its current size of 20,000 cells over 1 cm^2 would be straightforward and would not require more complex circuitry or multiple layers to avoid the crossing of leads. Because the microfabrication methods used to manufacture the device are routinely applied to regions of >100 cm^2, millions of cells could presumably be patterned by the same method.

In order to prevent the direct contact of cells with electrodes and to allow for a uniform surface chemistry between electrodes and non-electrode regions, we insulated the entire array surface with 200 Å of silicon dioxide. For other applications, different passivation layers could be used, or his layer could be omitted to allow direct contact between cells and electrodes.

Patterned adhesiveness was used to maintain the fidelity of cell patterns after cells adhered to the surface. To demonstrate one method of patterning adhesive surface chemistry, we adsorbed fibronectin, a cell-adhesive protein, through holes in membranes (Jackman et al., 1999) onto regions surrounding cell traps. Other methods of patterning

adhesiveness, such as microcontact printing and microfluidics, would also be applicable.

As with any system incorporating live cells, maintaining cell health is vital for the success of a new manipulation method. The 2 MHz, 5 V electrical field was shown both theoretically and experimentally to be nondamaging to the cells in our system. Propidium iodide dye exclusion demonstrated that at 10 V, membrane integrity was disrupted in cells. At 5 V, however, the system did not cause significant acute damage to cell membranes. Therefore, we proceeded to determine if this voltage produced any longer-term effects. Proliferation and cell morphology were used as broad indicators of cell health. Decreased proliferation could indicate an inability to complete the cell cycle, while an increase in cell proliferation could indicate cancerous transformation or other abnormal stimulation of growth pathways. Throughout the experiment, cells undergoing DEP proliferated at rates similar to those of tissue culture controls. The morphological similarity of cells undergoing DEP versus controls also rules out a variety of cellular maladies. While different cell types might have different thresholds for damage due to DEP, these thresholds are unlikely to vary greatly, since potential damage would likely occur as a dielectric breakdown of the cell membrane (Schwister and Deuticke, 1985), a structure common to all mammalian cells. We plan to test this assumption by using additional cell types in future experiments.

The points-and-lid DEP method was shown not only to be safe and effective, but also significantly more accurate than patterned adhesiveness, with correct patterning rates of 70 versus 17%, respectively. Although numerical comparison with all other techniques was beyond the scope of this paper, points-and-lid DEP compares favorably with a variety of methods. Microfluidics has been used to restrict cells to selected regions of a surface (Kane et al., 1999), but has not been able to prescribe the exact location of each cell in an array. Dielectrophoretic repulsion has been previously used to trap cells amongst post electrodes, which protruded from the substrate surface to trap single cells (Voldman et al., 2002). While this technique was shown to be effective for temporarily interrogating several cells with single-cell discrimination, it would be less practical for the generation of large arrays because it relies on a non-planar geometry and an intrinsically more complicated trapping process. Other electric positioning schemes have not demonstrated precise positioning of multiple single cells or prolonged pattern fidelity after cells adhered to the surface (Fuhr et al., 1994; Ozkan et al., 2003).

The improved patterning capabilities of points-and-lid DEP versus other systems would enable a variety of cell-based device applications by greatly improving manufacturing efficiency and precision. However, for some applications, an improvement over the current fidelity would be desirable. The main source of incorrect trapping appeared to be groups of cells, usually pairs of cells attached to each other, which were not separated during trypsinization. Therefore, an improved procedure to separate cells before use or to filter out attached pairs would greatly increase pattern fidelity. Lesser sources of error included defective traps and stochastic non-trapping, which could be reduced by improved fabrication and higher cell concentrations, respectively.

While the use of DEP trapping as demonstrated here could produce improved sensor output, independently controllable electrodes could enable new types of cell-based sensors that are unfeasible with current techniques. Electrodes not energized during DEP would not trap cells, and could provide the baseline signal for a sensor in the absence of cellular input. If traps left off during trapping of a first cell type were later energized, other cell types could be introduced in a controlled pattern relative to the first set of cells. While we have so far used DEP with only endothelial cells and fibroblasts, the success of other groups with manipulating a wide variety of cells (Pethig and Markx, 1997), and the electrical similarity of mammalian cells in general, implies that our technique would be applicable to many types of adherent cells. Patterning of multiple cell types could pave the way for densely packed sensors exposing several cell types to various stimuli. Multiple cell types in registration could also allow the introduction of support cells. For example, glial cells might be incorporated to support a functional nerve chip, providing a more physiological environment to neurons aligned with detectors. Neuron-based biosensors could also be constructed in a more sophisticated manner by utilizing the fact that DEP itself is orthogonal to the adhesiveness of the sensor surface. A sensor could be constructed such that DEP determined the locations and numbers of cell bodies, while adhesiveness determined the pattern of connections between neurons.

5. Conclusion

This work demonstrates the use of electrical forces to simultaneously position thousands of individual mammalian cells into a large array. Finite element modeling was used to guide the selection of design parameters and suggest the range of conditions under which the points-and-lid geometry can successfully trap single cells. Manipulating cells with DEP under appropriate conditions did not affect cell health, as demonstrated by a viability indicator and proliferation analysis. In a direct comparison, DEP was shown to have superior cell patterning accuracy versus the standard patterned-adhesiveness method. By combining electrical traps with aligned adhesive regions, we were able to maintain arrays of motile cells, which would otherwise crawl away from the traps after adhering to the surface. This combined method has the potential to facilitate the construction of a variety of biosensors and other cell-based devices by efficiently registering various types of cells with sensing and detecting elements. Cells could therefore be integrated into devices much like other components, by accurately specifying their number and locations.

Acknowledgements

The authors would like to thank D. Albrecht, S.N. Bhatia, C.M. Nelson, D.H. Reich, J. Tien, and L. Tung for helpful discussions and technical suggestions. This work was supported in part by the Whitaker Foundation, NIBIB (EB 00262), The Office of Naval Research, and DARPA.

References

Archer, S., Li, T.T., Evans, A.T., Britland, S.T., Morgan, H., 1999. Cell reactions to dielectrophoretic manipulation. Biochem. Biophys. Res. Commun. 257 (3), 687–698.

Ashkin, A., Dziedzic, J.M., Yamane, T., 1987. Optical trapping and manipulation of single cells using infrared laser beams. Nature 330 (6150), 769–771.

Balaban, N.Q., Schwarz, U.S., Riveline, D., Goichberg, P., Tzur, G., Sabanay, I., Mahalu, D., Safran, S., Bershadsky, A., Addadi, L., Geiger, B., 2001. Force and focal adhesion assembly: a close relationship studied using elastic micropatterned substrates. Nat. Cell Biol. 3 (5), 466–472.

Bhadriraju, K., Chen, C.S., 2002. Engineering cellular microenvironments to improve cell-based drug testing. Drug Discov. Today 7 (11), 612–620.

Djuzenova, C.S., Zimmermann, U., Frank, H., Sukhorukov, V.L., Richter, E., Fuhr, G., 1996. Effect of medium conductivity and composition on the uptake of propidium iodide into electropermeabilized myeloma cells. Biochim. Biophys. Acta 1284 (2), 143–152.

Docoslis, A., Kalogerakis, N., Behie, L., 1999. Dielectrophoretic forces can be safely used to retain viable cells in perfusion cultures of animal cells. Cytotechnology 30 (1–3), 133–142.

Freshney, R., 2000. Culture of Animal Cells, fourth ed. Wiley-Liss, New York.

Fuhr, G., Glasser, H., Muller, T., Schnelle, T., 1994. Cell manipulation and cultivation under a.c. electric field influence in highly conductive culture media. Biochim. Biophys. Acta 1201 (3), 353–360.

Galbraith, C.G., Sheetz, M.P., 1999. Keratocytes pull with similar forces on their dorsal and ventral surfaces. J. Cell Biol. 147 (6), 1313–1324.

Glasser, H., Fuhr, G., 1998. Cultivation of cells under strong ac-electric field—differentiation between heating and trans-membrane potential effects. Bioelectrochem. Bioenerg. 47 (2), 301–310.

Heida, T., Vulto, P., Rutten, W.L., Marani, E., 2001. Viability of dielectrophoretically trapped neural cortical cells in culture. J. Neurosci. Methods 110 (1/2), 37–44.

Huang, Y., Wang, X.B., Becker, F.F., Gascoyne, P.R., 1997. Introducing dielectrophoresis as a new force field for field-flow fractionation. Biophys. J. 73 (2), 1118–1129.

Hughes, M.P., Morgan, H., 1999. Measurement of bacterial flagellar thrust by negative dielectrophoresis. Biotechnol. Prog. 15 (2), 245–249.

Jackman, R.J., Duffy, D.C., Cherniavskaya, O., Whitesides, G.M., 1999. Using elastomeric membranes as dry resists and for dry lift-off. Langmuir 15 (8), 2973–2984.

Jager, E.W.H., Inganas, O., Lundstrom, I., 2000. Microrobots for micrometer-size objects in aqueous media: potential tools for single-cell manipulation. Science 288 (5475), 2335–2338.

Jones, T.B., 1995. Electromechanics of particles. Cambridge University Press, Cambridge.

Kane, R.S., Takayama, S., Ostuni, E., Ingber, D.E., Whitesides, G.M., 1999. Patterning proteins and cells using soft lithography. Biomaterials 20 (23/24), 2363–2376.

Murray, G.T.E., 1997. Handbook of Materials Selection for Engineering Applications. Marcel Dekker, Inc., New York, 280 pp.

Ozkan, M., Pisanic, T., Scheel, J., Barlow, S., Esener, S., Bhatia, S.N., 2003. Electro-optical platform for the manipulation of live cells. Langmuir 19 (5), 1532–1538.

Pancrazio, J.J., Whelan, J.P., Borkholder, D.A., Ma, W., Stenger, D.A., 1999. Development and application of cell-based biosensors. Ann. Biomed. Eng. 27 (6), 697–711.

Pethig, R., 1996. Dielectrophoresis: using inhomogeneous AC electrical fields to separate and manipulate cells. Crit. Rev. Biotechnol. 16 (4), 331–348.

Pethig, R., Markx, G.H., 1997. Applications of dielectrophoresis in biotechnology. Trends Biotechnol. 15 (10), 426–432.

Pohl, H.A., 1978. Dielectrophoresis: The behavior of Neutral Matter in Nonuniform Electric Fields, first ed. Cambridge University Press, New York.

Schwister, K., Deuticke, B., 1985. Formation and properties of aqueous leaks induced in human erythrocytes by electrical breakdown. Biochim. Biophys. Acta 816 (2), 332–348.

Sears, F.W., Zemansky, M.W., Young, H.D., 1980. University Physics, fifth ed. Addison-Wesley, Reading, MA, 465 pp.

Sison, E.S., Rahman, M.D., Durham, D.L., Hermanowski, J., Ross, M.F., Jennison, M., 1995. Dielectric and chemical characteristics of electron-beam-cured photoresist. Proc. SPIE 2438, 378–391.

Skerman, V.B., 1968. A new type of micromanipulator and microforge. J. Gen. Microbiol. 54 (2), 287–297.

Stenger, D.A., Gross, G.W., Keefer, E.W., Shaffer, K.M., Andreadis, J.D., Ma, W., Pancrazio, J.J., 2001. Detection of physiologically active compounds using cell-based biosensors. Trends Biotechnol. 19 (8), 304–309.

Tan, J.L., Tien, J., Pirone, D.M., Gray, D.S., Bhadriraju, K., Chen, C.S., 2003. Cells lying on a bed of microneedles: an approach to isolate mechanical force. Proc. Natl. Acad. Sci. U.S.A. 100 (4), 1484–1489.

Voldman, J., Braff, R.A., Toner, M., Gray, M.L., Schmidt, M.A., 2001. Holding forces of single-particle dielectrophoretic traps. Biophys. J. 80 (1), 531–541.

Voldman, J., Gray, M.L., Toner, M., Schmidt, M.A., 2002. A microfabrication-based dynamic array cytometer. Anal. Chem. 74 (16), 3984–3990.